Published in final edited form as:
J Neurovirol. 2010 April ; 16(2): 133–140. doi:10.3109/13550281003682547.

Varicella-zoster virus–induced apoptosis in MeWo cells is accompanied by down-regulation of Bcl-2 expression

Elizabeth Brazeau[1,2], **Ravi Mahalingam**[1], **Don Gilden**[1,2], **Mary Wellish**[1], **Benedikt B Kaufer**[3], **Nikolaus Osterrieder**[4], and **Subbiah Pugazhenthi**[5,6]

[1] Department of Neurology, College of Veterinary Medicine, Cornell University, Ithaca, New York, USA

[2] Department of Microbiology, College of Veterinary Medicine, Cornell University, Ithaca, New York, USA

[3] Department of Microbiology and Immunology, College of Veterinary Medicine, Cornell University, Ithaca, New York, USA

[4] Institut für Virologie, Freie Universität Berlin, Berlin, Germany

[5] Department of Medicine, University of Colorado School of Medicine, Aurora, Colorado, USA

[6] Veterans Administration Medical Center, Denver, Colorado, USA

Abstract

Varicella-zoster virus infects multiple human and monkey cells in culture. The mode of cell death appears to be autophagy or apoptosis. Analysis of VZV-infected human melanoma (MeWo) cells revealed that Bcl-2 mRNA and protein levels were decreased significantly 64 and 72 hpi (hours post infection), accompanied by the release of cytochrome c from mitochondria into the cytoplasm. Western blot analysis of virus-infected cells revealed activation of caspase-8, a marker for the extrinsic pathway of apoptosis, and caspase-9, a marker for the intrinsic pathway of apoptosis at 64 and 72 hpi. Significant increases in the levels of cleaved caspase-3 and cleaved poly (ADP) ribose polymerase (PARP) were also seen at the height of cytopathic effect. Thus VZV induces apoptosis in MeWo cells in which Bcl-2 is down-regulated. Future studies will determine differences in the cascade of apoptotic events in non-neuronal cells compared to neurons that allow VZV to become latent.

Keywords

apoptosis; Bcl-2; varicella-zoster virus

Introduction

Eukaryotic cells die either through necrosis or apoptosis. Apoptosis is a regulated suicide program characterized by chromatin condensation, DNA fragmentation, membrane blebbing, and cell shrinkage (Vaux *et al*, 1994). The induction of apoptosis can be brought about by different insults that include virus infection, ultraviolet (UV) irradiation, and deprivation of

Address correspondence to Dr. Don Gilden, Department of Neurology, University of Colorado Denver School of Medicine, 12700 E. 19th Avenue, Box B182, Aurora, CO 80045, USA., don.gilden@ucdenver.edu.

Declaration of interest: The authors report no conflicts of interest. The authors alone are responsible for the content and writing of the paper.

growth factors. Apoptosis is accompanied by activation of a cascade of cysteine-proteases called caspases followed by cleavage of poly (ADP) ribose polymerase (PARP) (Stennicke and Salvesen, 1998). Induction of apoptosis is mediated either through death receptors (extrinsic pathway) or at the mitochondrial level (intrinsic pathway). The intrinsic pathway involves regulation by the B-cell lym-phoma-2 (Bcl-2) family of proteins in mitochondria leading to activation of caspase-9 (Green and Reed, 1998), whereas the extrinsic pathway involves activation of caspase-8, which is initiated by the interaction of Fas ligand with death receptors (Ashkenazi and Dixit, 1998). Ultimately, both these processes result in activation of caspase-3. Bcl-2 proteins consist of antiapoptotic (Bcl-2, Bcl-xL, Mcl-1, and Bcl2A1) and proapoptotic multidomains (Bax and Bak1). An imbalance in the levels of these two groups of proteins leads to release of cytochrome *c* from mitochondria, which with Apaf-1 converts pro-caspase-9 to active caspase-9 (Green and Reed, 1998). In addition, BH3 (Bcl-2 Homology 3)–only proteins, a subset of proapoptotic proteins, act as sensors when cells are under stress (Huang and Strasser, 2000). These proteins are characterized by the presence of a 9–amino acid sequence BH3 region, as in the case of other Bcl-2 family members. BH3-only proteins include Bad, Bid, Bim, Bik, Bmf, Hrk, Noxa, and Puma. They induce apoptosis by either neutralizing antiapoptotic proteins or by activating proapoptotic proteins.

Varicella-zoster virus (VZV) causes chickenpox (varicella) in children, after which virus becomes latent in ganglia along the entire neuraxis (Gilden *et al*, 1983; Mahalingam *et al*, 1990, 1992). Decades later, virus reactivation produces shingles (zoster) and other neurological disorders in elderly and immunocompromised individuals. Although there have been reports of VZV-induced apoptosis in monkey kidney cells (Sadzot-Delvaux *et al*, 1995), in human fibroblasts (Hood *et al*, 2003), in peripheral blood mononuclear cells (PBMCs) isolated from healthy donors (König *et al*, 2003), and in PBMCs obtained from VZV-infected children (Pignata *et al*, 1998), the mechanism of apoptosis is unknown. The purpose of this study is to determine the mechanism of VZV-induced apoptosis in MeWo cells in culture.

Results and discussion

After VZV infection of MeWo cells by cocultivation, reverse transcriptase–polymerase chain reaction (RT-PCR) analysis revealed increased expression of VZV IE4, an immediate early transcript, 40 to 72 h post infection (hpi) (Figure 1A) in parallel with increases in levels of VZV glycoprotein E as shown by Western blot analysis (Figure 1B). Based on our earlier findings with simian varicella virus (SVV) (Pugazhenthi *et al*, 2009), we examined VZV-infected cells for Bcl-2 expression at the level of both transcription and translation. RT-PCR revealed a significant reduction of Bcl-2 mRNA levels 64 and 72 hpi in VZV-infected cells as compared to uninfected cells (Figure 2A). A decrease in Bcl-2 protein was also observed in VZV-infected cells as compared to uninfected cells at 64 and 72 hpi (Figure 2B, C). Finally, analysis of mitochondrial and cytoplasmic fractions of uninfected and VZV-infected cells revealed a substantial increase in release of cytochrome *c* from the mitochondria into the cytoplasm of virus-infected MeWo cells (Figure 3A–C).

To further determine the mechanism of VZV-induced cell death, infected cells were analyzed for markers of apoptosis. Western blot analysis revealed increase in the levels of active cleaved caspase-3 (Figure 4A) and accumulation of cleaved PARP (Figure 4B) at 64 and 72 hpi, at the height of cytopathic effect (CPE).

To facilitate investigation of the apoptotic potential of VZV, we constructed enhanced green fluorescent protein (EGFP)-labeled VZV. VZV ORF63 as well as ORF70 (duplicate copies of an immediate-early [IE] gene that are expressed throughout infection) were labeled with a C-terminal EGFP in an infectious BAC (bacterial artificial choromosome) clone of the P-Oka strain of VZV (Tischer *et al*, 2006, 2007). Resulting constructs were confirmed by PCR, DNA

sequencing, and multiple restriction fragment length polymorphisms (RFLPs) to ensure integrity of the genome. Identified clones were labeled as pORF63/70-EGFP (data not shown). Subsequently, these mutant BAC constructs were transfected into MeWo cells to produce recombinant VZV containing ORF63/70 fused to EGFP.

To determine if apoptosis is induced specifically in VZV-infected cells, MeWo cells infected by cocultivation with an EGFP-tagged VZV were examined by TUNEL (deoxynucleotidyltransferease-mediated dUTP nick end labeling) staining and by immunofluorescence. At 72 hpi, most infected cells (as evidenced by a cytopathic effect) were TUNEL-positive. Colocalization of EGFP with TUNEL staining revealed apoptosis in most virus-infected cells (Figure 5).

Apoptosis proceeds through extrinsic (death receptor) or intrinsic (mitochondrial) pathways. The intrinsic pathway proceeds through activation of capsase-9 and the extrinsic through activation of caspase-8. Modest activation of both caspase-8 and caspase-9 were detected in VZV-infected MeWo cells at 64 and 72 hpi (Figure 6A, B), suggesting the involvement of both pathways of apoptosis. The intrinsic pathway is regulated by the Bcl-2 family of proteins. Reduction in Bcl-2 expression further supports the role of intrinsic pathway in VZV-induced apoptosis.

The only other study that examined Bcl-2 expression in VZV-infected cells (Sadzot-Delvaux *et al*, 1995) reported that VZV-induced apoptosis was independent of Bcl-2, based on the qualitative detection of Bcl-2 transcripts by RT-PCR at one time point after VZV infection of monkey kidney cells. In contrast, our findings, which showed decreased levels of Bcl-2 mRNA and protein at multiple time points during progression of VZV infection, indicate an important role for Bcl-2 down-regulation in VZV-induced apoptosis. Analysis of Vero cells infected with SVV, the primate counterpart of human VZV, also showed decreased Bcl-2 expression and activation of caspase-9 (Pugazhenthi *et al*, 2009), indicating similarity in the pathways of induction of apoptosis by these closely related varicella viruses. Also, one or more proteins encoded by varicella probably influences transcription and translation of Bcl-2 as well as its inhibition of apoptosis. Bcl-2 expression is induced by the transcription factor cAMP response element–binding protein (CREB), which is activated by Akt and MAPK pathways (Pugazhenthi *et al*, 1999, 2000). Further studies are needed to determine if VZV infection interferes with CREB-mediated induction of Bcl-2.

The ability of VZV and SVV to induce apoptosis in MeWo and Vero cells, respectively, may be a cell type–specific phenomenon, as evidenced by the lack of detection of caspase-3 in VZV-infected MRC-5 cells undergoing autophagy (Takahashi *et al*, 2009). Although VZV induces apoptosis in non-neuronal cells, VZV becomes latent in neurons. Future studies will determine differences in the cascade of apoptotic events in non-neuronal cells compared to neurons that allow VZV to become latent.

Materials and methods

Generation of recombinant VZV

VZV ORF63 and ORF70 of pP-Oka, an infectious bacterial artificial chromosome (BAC) clone of the P-Oka strain, was labeled with a C-terminal enhanced green fluorescent protein (EGFP) using two-step red-mediated mutagenesis as described (Tischer *et al*, 2006, 2007). Briefly, the EGFP-I-*Sce*I-*aphAI* cassette was amplified from pEP-EGFP in plasmid DNA with primers *63/70EGFP for*, GTCGACACGAAGCCCCGCGCCGGCATGATATACCGCCCCCCCATGGCGTGGTGAGCAAGGGCGAGGAGCT, and *63/70EGFP rev*, ACATCAAAAAAAGACACGAGCCAAACCATTGTATTTATTTATAAAGACTACTTG

TACAGCTCGTCCATGCCG, and introduced into pP-Oka (Tischer *et al*, 2007) via red recombination in GS1783 *Esherichia coli* cells (kindly provided by Gregory A. Smith, Northwestern University, Chicago, IL). Resulting clones were characterized by restriction fragment length polymorphism (RFLP) analyses and correct clones were selected for the second recombination procedure. Final clones were analyzed by RFLP, PCR, and DNA sequencing to confirm the correct fusion of EGFP as well as the integrity of the recombinant BAC construct.

Reconstitution of VZV from BAC DNA

BAC DNA used for transfection was isolated using the Qiagen Midiprep kit according to the manufacturer's instruction. Subsequently, human malignant melanoma (MeWo) cells were transfected with the BAC clone using Lipofectamine 2000 (Invitrogen, Carlsbad, CA). Briefly, 1 μg recombinant BAC DNA was cotransfected with 200 ng pCMV62, a plasmid containing the VZV IE gene ORF62 under control of a cytomegalovirus (CMV) promoter. The DNA-lipofectamine solution was added onto cells and incubated for 4 h. The transfection medium was replaced with growth medium, as per the manufacturer's instructions. The recombinant VZV expressing ORF63 fused to EGFP was identified with a fluorescence microscope.

Cells and virus

The Ellen strain of VZV was propagated in MeWo cells in Dulbecco's modified Eagle's medium (Invitrogen) supplemented with 10% heat-inactivated fetal calf serum, 1% penicillin/streptomycin, and 1% L-glutamine at 37°C in 5% CO_2 by cocultivation of infected cells with uninfected cells at a ratio 1:32. Wild-type and EGFP-labeled VZV virus were passaged in MeWo cells by cocultivation of infected with uninfected cell at a ratio of 1:2 to 1:5.

Quantitative RT-PCR

Uninfected or VZV infected MeWo cells were trypsinized and centrifuged at 1000 × *g* for 5 min. Total RNA was extracted from the pellets with the RNeasy minikit (Qiagen, Valencia, CA) and quantitated using a Nano-drop ND-1000 spectrophotometer. Total RNA (2 μg) was treated in a 20-μl volume with 1 unit of Amplification grade DNase I (Invitrogen) and reverse transcribed using the First Strand cDNA Synthesis Transciptor kit (Roche, Indianapolis, IN) as per the manufacturer's instructions. cDNA was analyzed by quantitative RT-PCR for the VZV IE4 transcript using the 7500 Fast Real Time PCR System from Applied Biosystems (Foster City, CA). The real-time PCR reaction was performed in a total volume of 20 μl containing 1× master mix of Absolute QPCR lowRox Mix (Thermo Scientific, Waltham, MA), 900 nM of each primer, 250 nM VZV IE4 probe, and 5 μl cDNA. Amplification conditions included denaturation at 95°C for 15 min, followed by 50 two-step cycles of 95°C for 15 s and 60°C for 1 min. Samples were analyzed in triplicate. Primers and Taqman probe were as follows: VZV VZV IE 4 forward primer 5′-ATGGCGTACCGAGTCAATGG-3′; VZV IE4 reverse primer primer 5′-GCCGTGCTATTGAAGTCGTCT-3′; Taqman probe 6FAM 5′-ACCGCGGGAGCCAGCGTG-3′ TAMARA. Primers and probe were generated by Applied Biosystems. The VZV IE4 amplicon (5′-GCCGTGCTATTGAAGTCGTCTCCACCGCGGGAGCCAGCGTGACCATTGACTCGGTACGCCAT-3′), obtained from Integrated DNA Technologies (Iowa City, IA), was used to generate a standard curve.

TUNEL staining

The ApopTag Red In Situ Apoptosis Detection Kit (Chemicon International, Temecula, CA) was used to stain for TUNEL-positive cells per manufacturer's instructions. Uninfected and VZV-EGFP–infected cells at 48 and 72 h post infection (hpi) by cocultivation were washed in phosphate-buffered saline (PBS) and fixed in 1% paraformaldehyde in PBS, followed by

permeabilization with 2:1 ethanol/acetic acid at −20°C for 5 min. Cells were incubated with TdT enzyme at 37°C for 1 h, followed by three washes with PBS. Cells were then incubated with rhodamine-conjugated anti-digoxigenin antibody in the dark at room temperature for 30 min, followed by four PBS washes. Coverslips were mounted with Vectashield mounting medium containing DAPI (4′,6-diamidino-2-phenylindole) (Vector Labs, Burlingame, CA) and visualized with a Zeiss Axioplan 2 EPI Fluorescence upright Digital Deconvolution microscope. TUNEL staining was performed twice.

Western blots

Uninfected or VZV-infected cells were washed with ice-cold PBS and scraped into lysis buffer (150 nM NaCl, 1 mM EDTA, 1 mM EGTA, 5 mM sodium pyrophosphate tetrabasic decahydrate, 1 mM sodium orthovanadate, 20 mM sodium fluoride, 500 nm okadaic acid, and 1 ml protease inhibitor [P8340; Sigma, St. Louis, MO]). Cells were agitated for 30 min at 4° C and centrifuged at 10,000 × *g* for 10 min at 4°C.

Supernatants were quantitated using the Bradford assay. Protein lysates (2 μl) were added to 100 μl of Bradford assay reagent (1700 ml dH_2O, 200 ml ortho-phosphoric acid, 100 ml 95% ethanol, and 200 mg Coomasie Brilliant Blue) and measured on a Bio-Rad Microplate Reader at 595 nm. Protein concentration was determined by comparison to a standard curve generated by diluting known amounts of protein (bovine serum albumin [BSA]) into Bradford reagent.

To test for caspase-3, −8, −9, PARP, cytochrome *c*, and VZV glycoprotein E (gE), 30 μg of VZV-infected or unifected cell lysates was loaded per well and 5 μg for detection of Bcl-2. Criterion Precast Tris HCl 10% Resolving Gels were used (Bio-Rad, Hercules, CA) with Precision Plus Protein Kaleidoscope Standard (Bio-Rad) to indicate protein size. Protein was transferred onto an Immobilon P Membrane (Millipore, Bedford, MA). The membrane was blocked with 6% nonfat dry milk in 0.1% Tween-20 TBS (Tris buffered saline, 50 mM Tris, 150 mM NaCl) at room temperature for 1 h, followed by incubation with primary antibody. The primary antibodies (all purchased from Cell Signaling Technologies, Boston, MA) used were rabbit anti-cleaved caspase-3 (catalog no. 9661; 1:1000 dilution), or rabbit anti-cleaved caspase-8 (catalog no. 9496; 1:1000 dilution), rabbit anti-cleaved PARP (catalog no. 9541; 1:1000 dilution), or rabbit anti-VDAC (voltage dependent, ion selective channel) (catalog no. 4866; 1:500 dilution), or rabbit anti-cytochrome *c* (catalog no. 4280; 1:500 dilution), or rabbit anti-Bcl-2 (catalog no. 2780; 1:1000 dilution); other primary antibodies used were rabbit anti-cleaved caspase-9 (Calbiochem, San Diego, CA; catalog no. AP1014; 1:500 dilution), or mouse anti-VZV gE antibody (Santa Cruz Biotechnology, Santa Cruz, CA; catalog no. sc-56994; 1:1000 dilution), or mouse anti-β-actin antibody (Sigma, catalog no. A5441; 1:1000 dilution). After incubation with primary antibody in 5% BSA/TBST overnight at 4°C, the membranes were washed in 6% nonfat dry milk in TBST three times for 5 min each time, followed by incubation with secondary antibody.

Secondary antibodies, diluted in 6% nonfat dry milk in TBST, were either alkaline phosphatase–conjugated anti-rabbit Ig H+L (Vector Labs, catalog no. AP-1000; 1:1000 dilution) or alkaline phosphatase–conjugated anti-mouse Ig H+L (Vector Labs, catalog no. AP-2000; 1:1000 dilution). Membranes were incubated with secondary antibody for 1 h at room temperature, followed by three washes in 6% nonfat dry milk in TBST for 5 min each time and two washes in 10 10 mM Tris-HCl, 10 mM NaCl, 1 mM $MgCl_2$ (pH 9.5) for 5 min each time. Membranes were then immersed in a 1:500 dilution of CDP-Star Reagent in 1× CDP-Star Assay Buffer (New England Biolabs, Ipswich, MA) and incubated for 5 min at room temperature, followed by exposure to Kodak X-OMAT film (Fisher Scientific, Pittsburgh, PA) and developed using a Kodak X OMAT 1000 processor.

Stripping of blots

Blots were treated using Restore PLUS Western Blot Stripping Buffer (Thermo Scientific) for 20 min at room temperature with gentle rocking, rinsed for 5 min with TBST at room temperature, followed by blocking with 6% nonfat dry milk in TBST for 1 h at room temperature.

Densitometric analysis

Western blots containing Bcl-2 and β-actin bands were scanned using a Microtek ScanMaker i800 scanner digital film and photo scanner. Densitometry analysis was performed using Image Quant software (GE Healthcare, Piscataway, NJ).

Cytochrome c assay

Uninfected and VZV-infected MeWo cells were harvested at 48 and 72 hpi. The ProteoExtract Cytosol/ Mitochondria Fractionation kit (Calbiochem) was used to isolate mitochondria and cytosol. Cells were trypsinized and centrifuged at 600 × *g* for 5 min at 4°C. Cell pellets were washed with cold PBS, centrifuged at 600 rpm for 5 min at 4°C, resuspended in cytosol extraction buffer mix (kit component), and incubated on ice for 10 min. Cells were lysed by dounce homogenization (50 strokes) on ice and centrifuged at 700 × *g* for 10 min at 4°C to remove cell debris. Cytosolic and mitochondrial fractions were separated by centrifugation at 10,000 × *g* for 30 min at 4°C. The supernatant was removed (cytosolic fraction) and the pellet (mitochondrial fraction) was resuspended in mitochondrial extraction buffer mix (kit component). Protein concentrations were normalized using the Bradford assay and analyzed by Western blot as described above. Membranes were first probed for cytochrome *c*, stripped, and reprobed for VDAC, restripped, and reprobed for β-actin.

Acknowledgments

This work was supported in part by Public Health Service grants NS032623 and AG006127 (D.H.G. and R.M.) and AG032958 (D.H.G., R.M., S.P.) from the National Institutes of Health. Elizabeth Brazeau was supported by NIH Public Health Service Training Grant NS007321. The authors thank Dr. Randall Cohrs for useful discussions and Cathy Allen for manuscript preparation.

References

Ashkenazi A, Dixit VM. Death receptors: signaling and modulation. Science 1998;281:1305–1308. [PubMed: 9721089]

Gilden DH, Vafai A, Shtram Y, Becker Y, Devlin M, Wellish M. Varicella-zoster virus DNA in human sensory ganglia. Nature 1983;306:478–480. [PubMed: 6316159]

Green DR, Reed JC. Mitochondria and apoptosis. Science 1998;281:1309–1312. [PubMed: 9721092]

Hood C, Cunningham AL, Slobedman B, Boadie RA, Abendroth A. Varicella-zostervirus-infectedhuman sensory neurons are resistant to apoptosis, yet human foreskin fibroblasts are susceptible: evidence for a cell-type-specific apoptotic response. J Virol 2003;77:12852–12864. [PubMed: 14610206]

Huang DC, Strasser A. BH3-only proteins-essential initiators of apoptotic cell death. Cell 2000;103:839–842. [PubMed: 11136969]

König A, Homme C, Hauröder B, Dietrich A, Wolff MH. The varicella-zoster virus induces apoptosis in vitro in subpopulations of primary human peripheral blood mononuclear cells. Microbes Infect 2003;5:879–989. [PubMed: 12919856]

Mahalingam R, Wellish M, Wolf W, Dueland AN, Cohrs R, Vafai A, Gilden DH. Latent varicella-zoster virus DNA in human trigeminal and thoracic ganglia. N Engl J Med 1990;323:627–630. [PubMed: 2166914]

Mahalingam R, Wellish M, Dueland AN, Cohrs R, Gilden DH. Localization of herpes simplex virus type 1 and varicella-zoster virus in human ganglia. Ann Neurol 1992;31:444–448. [PubMed: 1316733]

Pignata C, Fiore M, de Filipppo S, Cavalcanti M, Gaetaniello L, Scotese I. Apoptosis as a mechanism of peripheral blood mononuclear cell death after measles and varicella-zoster virus infections in children. Pediatr Res 1998;43:77–83. [PubMed: 9432116]

Pugazhenthi S, Miller E, Sable C, Young P, Heidenreich KA, Boxer LM, Reusch JE. Insulin-like growth factor-I induces bcl-2 promoter through the transcription factor cAMP-response element-binding protein. J Biol Chem 1999;274:27529–27535. [PubMed: 10488088]

Pugazhenthi S, Gilden DH, Nair S, McAdoo A, Wellish M, Brazeau E, Mahalingam R. Simian varicella virus induces apoptosis in monkey kidney cells by the intrinsic pathway and involves downregulation of Bcl-2 expression. J Virol 2009;83:9273–9282. [PubMed: 19605493]

Pugazhenthi S, Nesterova A, Sable C, Heidenreich KA, Boxer LM, Heasley LE, Reusch JE. Akt/protein kinase B up-regulates Bcl-2 expression through cAMP-response element-binding protein. J Biol Chem 2000;275:10761–10766. [PubMed: 10753867]

Sadzot-Delvaux C, Thonard P, Schoonbroodt S, Piette J, Rentier B. Varicella-zoster virus induces apoptosis in cell culture. J Gen Virol 1995;76:2875–2879. [PubMed: 7595398]

Stennicke HR, Salvesen GS. Properties of the caspases. Biochim Biophys Acta 1998;1387:17–31. [PubMed: 9748481]

Takahashi MN, Jackson W, Laird DT, Culp TD, Grose C, Haynes JI II, Benetti L. Varicella-zoster virus infection induces autophagy in both cultured cells and human skin vesicles. J Virol 2009;83:5466–5476. [PubMed: 19297471]

Tischer BK, Kaufer B, Sommer M, Wussow F, Arvin AM, Osterrieder N. A self-excisable infectious bacterial artificial chromosome clone of varicella-zoster virus allows analysis of the essential tegument protein encoded by ORF9. J Virol 2007;81:13200–13208. [PubMed: 17913822]

Tischer BK, von Einem J, Kaufer B, Osterrieder N. Two-step red-mediated recombination for versatile high-efficiency markerless DNA manipulation in Escherichia coli. Biotechniques 2006;40:191–197. [PubMed: 16526409]

Vaux DL, Haecker G, Strasser A. An evolutionary perspective on apoptosis. Cell 1994;76:777–779. [PubMed: 8124715]

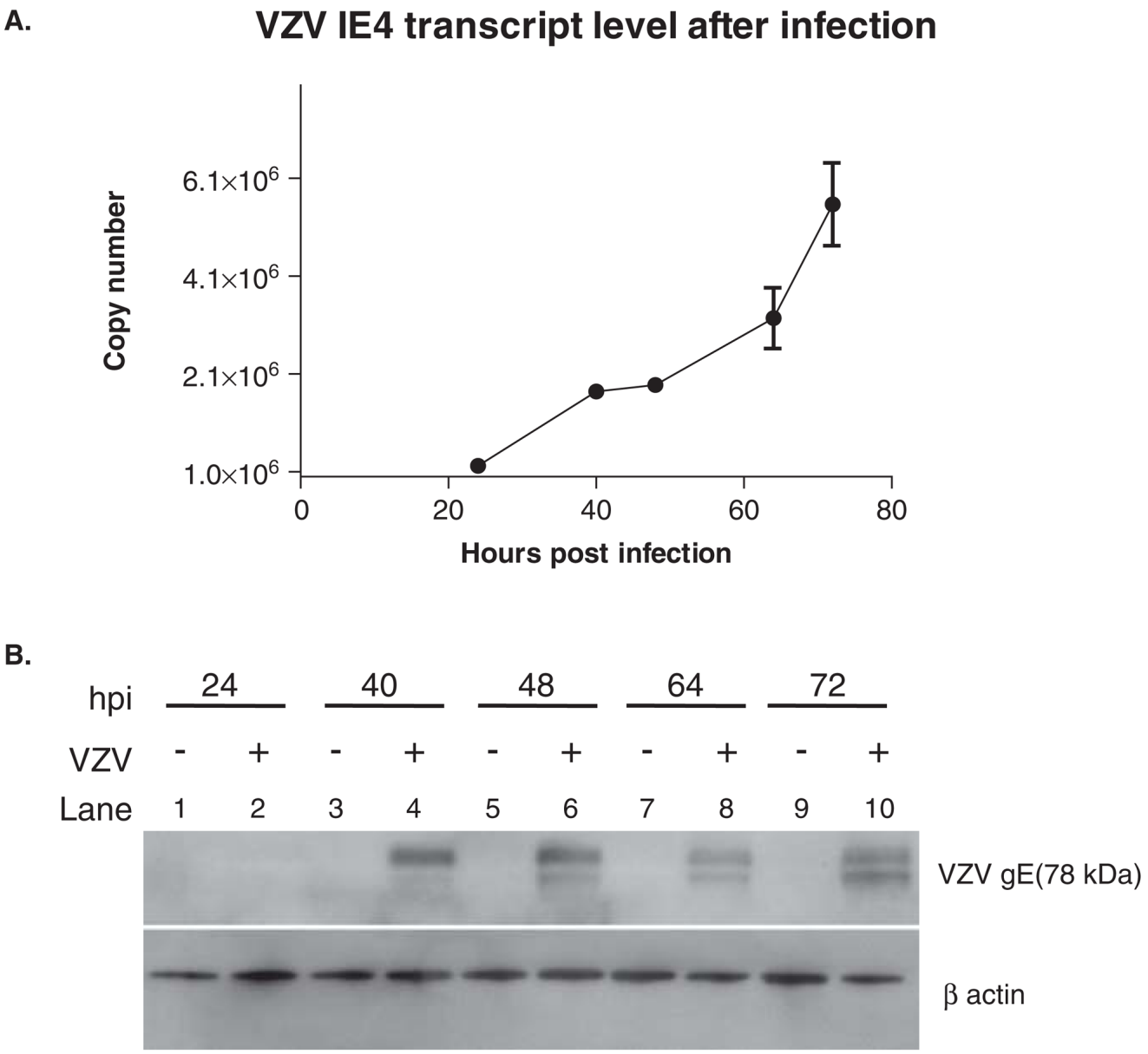

Figure 1.

Detection of VZV IE 4 transcripts by qRT-PCR and VZV glycoprotein E by Western blot analysis in VZV-infected MeWo cells. Total DNase-treated RNA was reverse-transcribed and analyzed by PCR at multiple times after infection for VZV immediate-early (IE) 4 transcripts. No VZV IE4 transcripts were found in uninfected cells (data not shown), whereas infected cells had increasing amounts of transcript over 72 h (**A**). Lysates of uninfected and VZV-infected cells were also analyzed at the same times as described in Materials and Methods for the presence of VZV glycoprotein E (78 kDa) and β-actin. VZV glycoprotein E was found 40 to 72 h post infection (hpi) (**B**).

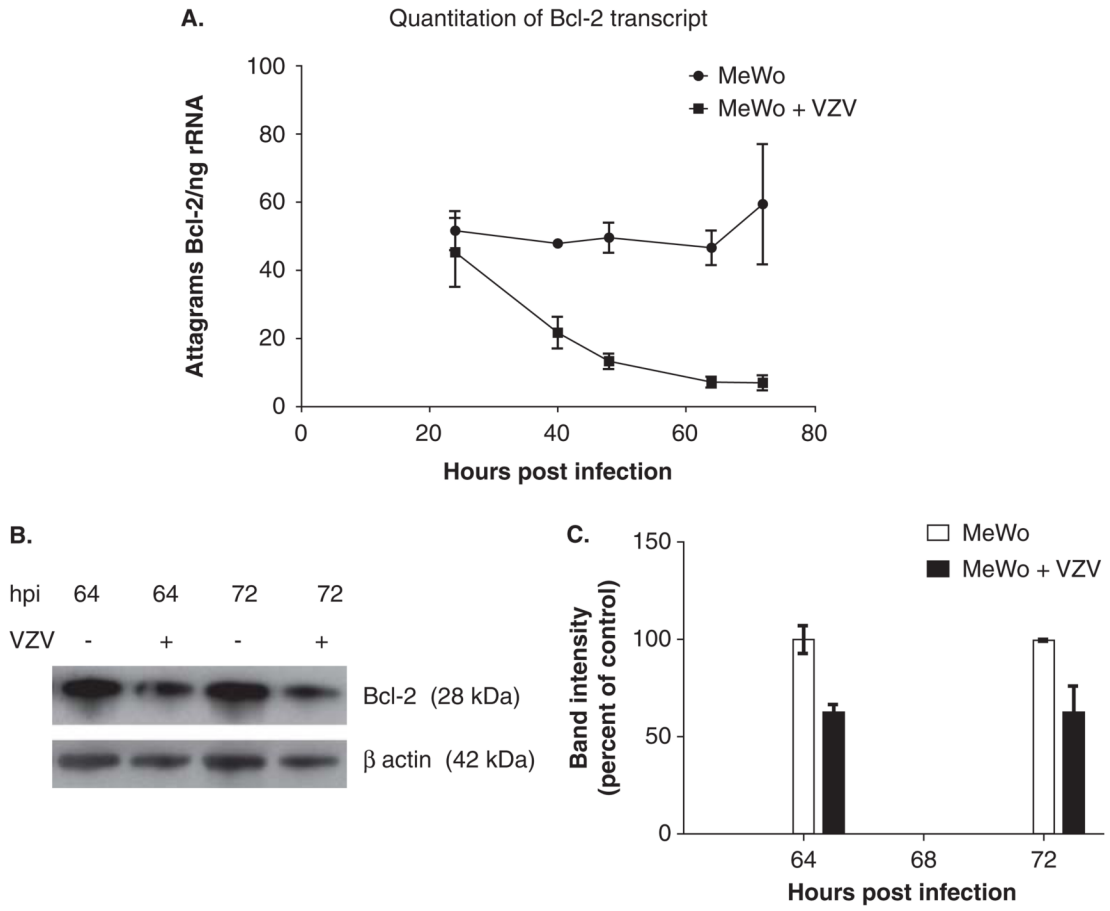

Figure 2.

Analysis of Bcl-2 transcript and protein levels. Total DNase-treated RNA was reverse-transcribed and analyzed by PCR at multiple times after infection for Bcl-2 and ribosomal RNA transcripts. Compared to uninfected MeWo cells, the amount of Bcl-2 transcript normalized to ribosomal RNA decreased over the course of infection (**A**). Lysates of uninfected and VZV-infected cells were also analyzed by Western blot for Bcl-2 protein. From 64 to 72 hpi, there was a reduction in the amount of the anti-apoptotic protein Bcl-2 as compared to uninfected cells (**B**). Bcl-2 protein levels (normalized to β-actin) were determined by densitometric analysis of blots in panel **B** and were lower in VZV-infected cells 64 and 72 hpi (**C**).

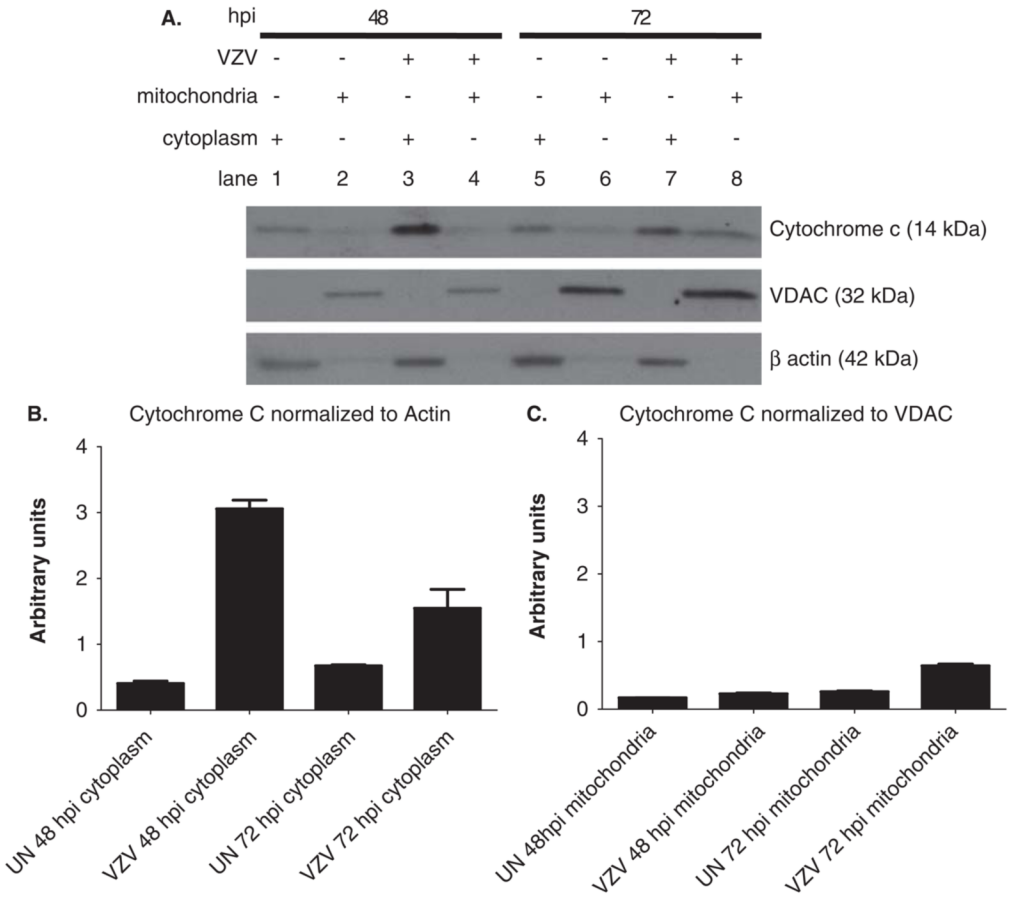

Figure 3.

Release of cytochrome *c* into the cytoplasm of VZV-infected MeWo cells. Mitochondrial and cytoplasmic fractions from uninfected and VZV-infected cells were analyzed at 48 and 72 hpi for cytochrome *c*. At 48 hpi, cytochrome *c* was seen in the cytoplasm of VZV-infected cells (**A**, lane 3). Detection of the mitochondrial protein VDAC (32 kDa) and β-actin (42 kDa) at 48 and 72 hpi confirmed the integrity of mitochondrial and cytoplasmic fractions (lower panels in **A**). Cytochrome *c* levels in the cytoplasm (normalized to β-actin) determined by densitometric analysis of blots in panel A were higher in VZV-infected cells at 48 and 72 hpi than in uninfected cells (**B**). Cytochrome *c* levels in the mitochondria (normalized to VDAC) determined by densitometric analysis of blots in panel **A** were not significantly different between VZV- infected and uninfected cells (**C**).

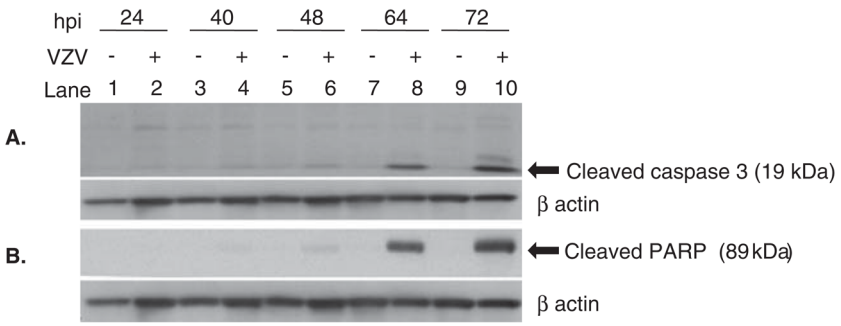

Figure 4.

Detection of cleaved caspase-3 and PARP in VZV-infected MeWo cells. Uninfected and VZV-infected MeWo cell lysates were analyzed by Western blot for markers of apoptosis (cleaved caspase-3 and cleaved PARP) as described in Materials and Methods. The active cleaved caspase-3 (19 kDa) was detected beginning 48 h post infection (hpi) and increasing up to 72 hpi, the height of the VZV-induced cytopathic effect (lanes 6, 8, and 10) (**A**). Cleaved PARP (89 kDa), indicating the final stages of apoptosis, increased from 64 and 72 hpi (lanes 8 and 10) (**B**). To ensure equivalent loading of protein, both blots were stripped and reprobed for β-actin (lower panels in **A** and **B**).

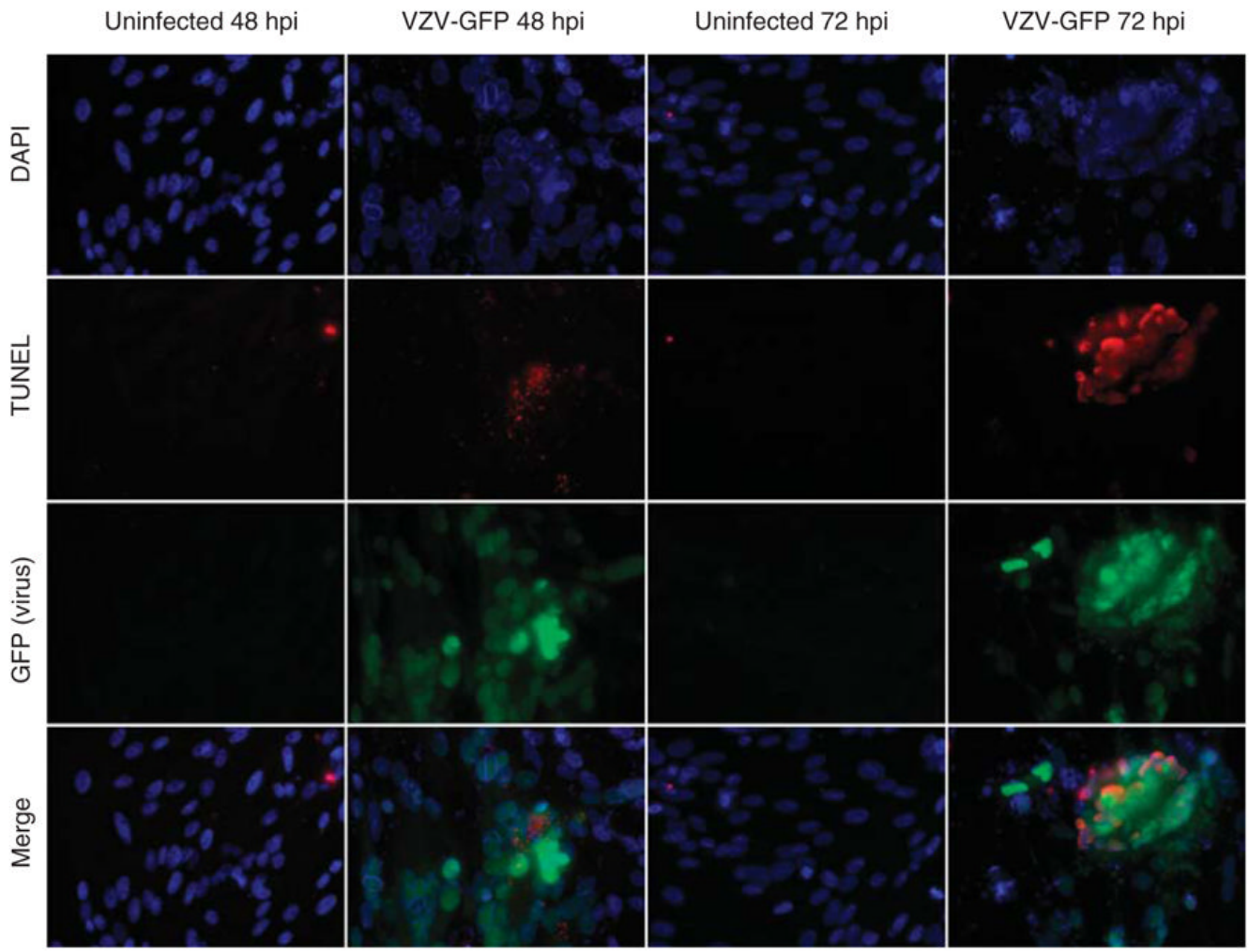

Figure 5.

Detection of apoptosis in VZV-infected MeWo cells. VZV-infected MeWo cells expressing EGFP were fixed at 48 or 72 h post infection (hpi) and examined by TUNEL assay. DAPI staining (blue color) reveals nuclei. Red fluorescence reveals TUNEL-positive cells that increased from 48 and 72 hpi, confirming apoptosis. Green fluorescence shows VZV-infected cells 48 and 72 hpi. VZV colocalized with TUNEL-positive cells 48 and 72hpi (bottom row).

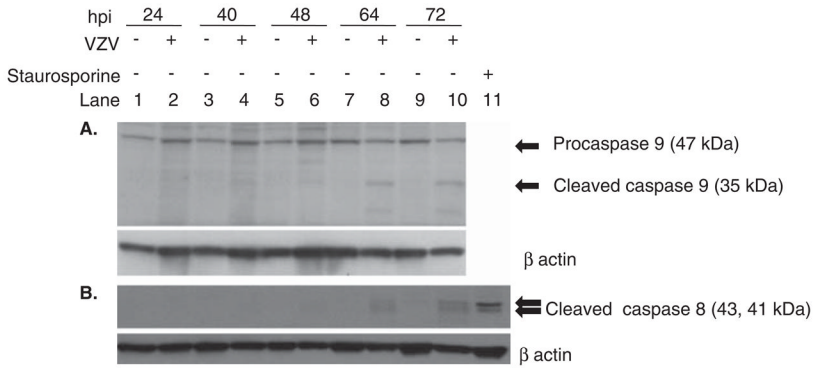

Figure 6.

Analysis of uninfected and VZV-infected MeWo cells for caspase-9 and -8. Uninfected and VZV-infected cells were analyzed by Western blot for caspase-9 and -8. Procaspase-9 (47 kDa) was detected at all time points. Cleaved caspase-9 (35 kDa) was seen beginning 64 h post infection (hpi) (lane 8) and increased by 72 hpi (lane 10) (**A**). Cleaved caspase-8 (43 and 41 kDa) was detected after treatment of cells for 5 5 h with the protein kinase C inhibitor staurosporine (lane 11). At the height of a VZV-induced cytopathic effect (72 hpi), trace amounts of cleaved caspase-8 was detected in VZV-infected cells (lane 10). To ensure equivalent loading of protein, both blots were stripped and reprobed for β-actin (lower panels in **A** and **B**).